JOINT EUROPEAN TORUS

JET–P(91)19

M. Danielsson, M.G von Hellermann, E. Kallne, W. Mandl, H.W. Morsi,
H.P. Summers, K-D Zastrow and JET Team

On Comparison of Spectroscopically Deduced Central Ion Temperatures and Plasma Rotation at JET

On Comparison of Spectroscopically Deduced Central Ion Temperatures and Plasma Rotation at JET

M. Danielsson[1], M.G von Hellermann, E. Kallne[1], W. Mandl, H.W. Morsi, H.P. Summers, K-D Zastrow[1] and JET Team*

JET-Joint Undertaking, Culham Science Centre, OX14 3DB, Abingdon, UK

[1]Department of Physics I, Royal Institute of Technology, Stockholm, Sweden
** See Appendix 1*

Preprint of Paper to be submitted for publication in
Review of Scientific Instruments

On comparison of spectroscopically deduced central ion temperatures and plasma rotation at JET

M. Danielsson[†], *M.G. vonHellermann, E. Källne*[†]
W. Mandl, H.W. Morsi, H.P. Summers, K.-D. Zastrow[†]

JET Joint Undertaking
Abingdon GB-OX14 3EA
[†]Department of Physics I, Royal Institute of Technology
S-10044 Stockholm

Abstract

It is shown that a significant increase in the consistency of charge exchange spectroscopy and x-ray spectroscopy deduction of central ion temperature and plasma rotation is obtained when allowance is made for the following:

i. The charge exchange cross section dependence on the impact energy of the neutral beam atoms in the frame-of-reference of the C^{+6} nuclei. In this paper we have experimentally verified the predicted cross section effects on ion temperature and plasma rotation measurements by comparing to passive x-ray spectroscopy. The effect increases with lighter species.

ii. The precise position of the radiating ion shell in line-of-sight averaged measurements using x-ray spectroscopy. For high temperature plasmas with broad emission profiles the uncertainty in central ion temperature is reduced from up to 60 % to the order of 20 %.

1.0 Introduction

Spectroscopic deductions of ion temperature have not proved consistent at the accuracy levels required for this stage in the fusion programme (Morsi et al. 1990). Since spectroscopic methods, in spite of this, are considered to be the only reliable way of determining this crucial plasma parameter, improvements of the accuracy are highly desirable. Recently also the importance of accurate plasma rotation measurements has increased. For example the proposed change of poloidal rotation during a phase transition of the plasma from L-mode to H- mode is only of the order 1 krad/s (Groebner et al. 1989, 1990, Shaing et al. 1989, Biglari et al. 1990). Also of interest is the linear relationship between ion temperature and rotation frequency (de Esch et al. 1990). From this relationship it is possible to deduce plasma parameters such as heat and momentum diffusivity. Finally, the possible correlation between the frequency of MHD activity and plasma rotation, for example during locked modes, is attracting attention (Snipes et al. 1990, Nave et al. 1991).

Spectroscopic measurements of plasma rotation and ion temperature at the JET tokamak are based on active charge exchange spectroscopy (Weisen et al. 1989) and high resolution x-ray spectroscopy (Bombarda et al. 1989). The advantage with the former system is that its observation volume is localized at the intersection of the neutral beam and the line-of-sight, whilst the latter passive system detects whole line-of-sight integrated emission. In the present study helium-like nickel (Ni^{+26}) x-ray spectra are used together with charge exchange recombination spectra from the (C^{+5}) n=8 to n=7 transition.

From the charge exchange cross section dependence on impact energy a shift and a change in the width of the observed charge exchange spectral lines are predicted. For the JET viewing line geometry (figure 1) this will lead to a red shift and a decreased width of the observed charge exchange spectrum, which, if not corrected for, results in an underestimated ion temperature and rotation frequency of the plasma. In order to see if this can be verified, experimental data from the charge exchange multichord system are compared with experimental data from the x-ray crystal spectrometer. To make this comparison meaningful it has to be taken into account that the observed x-ray emission spectrum is a composite spectrum which is the result of integrating the emissivity along the line-of-sight. Radial profiles of the electron temperature and density

as well as the gradients of the radial profiles of toroidal rotation and ion temperature determine the actual spectral shape (Zastrow et al. 1991).

The comparison confirms the theoretical prediction of apparent ion temperatures and plasma rotation deviating from the true values. The deviations, which depend on the ion temperature, are typically 5 % for the ion temperature and 10 % for the rotation frequency. For example for a 5 keV plasma in locked mode the rotation frequency is corrected from being apparently zero to a real rotation frequency of about 5 krad/s in the direction of the plasma current.

When trying to measure the change in poloidal rotation connected with L-mode to H-mode transitions (Groebner et al. 1989, 1990) the cross section effects must be considered, because the transition also involves a change in ion temperature. The peak shift due to cross section effects is here of the same order as the observed peak shift from which a change in poloidal rotation has been deduced.

2.0 Experiment

The charge exchange multichord system (CXRS)

Neutral beam injection is routinely used at JET to heat the plasma. Since the neutral beams are arranged according to figure 1 they will also transfer momentum to the plasma, which causes the plasma rotation. The active charge exchange spectroscopy diagnostic is based on observing emission lines produced by charge exchange from the deuterium atoms in the neutral beam with impurity ions, such as carbon and beryllium, which are present in the plasma. The data in this work are based on observations of the charge exchange recombination C^{+5} n=8 to n=7 transition at $\lambda_0 = 5290.5$ Å. The halfwidth, $\delta\lambda$, of the line determines the ion temperature T_i through the relationship:

$$\frac{\delta\lambda}{\lambda_0} = constant \cdot \sqrt{\frac{T_i}{M_c}} \qquad [1]$$

where M_c is the mass of the carbon ion.

The rotation velocity v is determined through the Doppler shift $\Delta\lambda$ of the observed line:

$$v = c \cdot \frac{\Delta\lambda}{\lambda_0} \qquad [2]$$

The shift in wavelength, $\Delta\lambda$, is measured by a comparison of the position of a line from cold C^{+5} at the edge of the plasma. After the introduction of beryllium into the tokamak during 1989 a line emitted from cold non-rotating beryllium ($Be^{+1}\lambda = 5271.5$ Å) with a temperature of about 10 eV (figure 3) has, if possible, been used as a reference. This improves the accuracy of the wavelength shift measurement since the beryllium ions are closer to the plasma boundary than the carbon

ions. For very hot and fast rotating plasmas the emisssion shell of carbon at the plasma edge can rotate and the position of the cold carbon line will be shifted. In figure 3 it can be seen that this is clearly the case, and the carbon line cannot be used as a reference.

The light is collected by an array of up to 12 optical quartz fibres, each collecting the light from a specific point along the neutral beam according to figure 2. The 90 m long optical fibres end at a Czerny-Turner spectrometer (SPEX 1269) equipped with a vidicon array of 500 x 512 pixels. Thus, 8 to 12 spectra from different points along the major radius (figure 2) are simultaneously recorded. The exposure time is 50 ms and the readout time is 50 ms which gives a time resolution of about 100 ms. The spectrometer grating of 600 lines/mm provides a dispersion at the vidicon of 0.325 Å/pixel at a centre wavelength of 5290.5 Å. The resolution $\lambda/\Delta\lambda$ is therefore about 16000. The central wavelength which determines the Doppler shift has a typical statistical error of $\pm$ 0.2 Å, due to the fact that approximately 200 pixels are used for an entire spectral profile. When the beryllium line is used as a reference the accuracy is better than 0.1 Å. As a comparison line shifts are of the order 5 Åand half widths (FWHM) of the order 10 Å.

The high resolution x-ray crystal spectrometer (XCS)

The high resolution x-ray crystal spectrometer (XCS) records the resonance line in helium-like nickel, i.e. the $1s2p\,^1P_1 \rightarrow 1s^2\,^1S_0$ transition. This line is used since, for electron temperatures at JET, it is the strongest x-ray line. Resonance lines from hydrogen-like nickel are, for example, too weak. The width of this line gives the ion temperature T_i whilst the shift in peak position of the line gives the rotation velocity.

The lay-out of the x-ray crystal spectrometer is shown in figure 1. It is of Rowland circle geometry with a radius of about 20 m giving a resolution as good as 20000. This means, for example, that it is possible to detect changes in the rotation frequency of only 3 krad/s (Eriksson et al. 1991) corresponding to 0.03 mÅ (which is about 0.75 % of the typical FWHM). The best time resolution of the system is 20 ms, but depends on the count rate statistics required for the analysis.

3.0 Analysis of data

Cross section effects on charge exchange spectroscopy

The charge exchange spectroscopy is based on charge transfer from the deuterium atoms in the neutral beam to the impurity ions in the plasma. The reaction considered here is:

$$D^0 + C^{6+} \rightarrow D^+ + C^{5+}(n = 8) \qquad [3]$$

$$C^{5+}(n = 8) \rightarrow C^{5+}(n = 7) + h\nu$$

For the C^{5+} ion the light from the n=8 to n=7 transition is observed. The effective emission cross section for this reaction depends on the impact energy of the D^0 atoms in the frame of reference of the C^{6+} ions. For a given ion temperature an approximation of the cross section variation over the range of thermal velocities of ions representing a full spectrum is described by:

$$\sigma(v_{rel}) = \sigma_0 + \frac{\partial\sigma}{\partial v_{rel}} \cdot \Delta v_{rel} + \frac{\partial^2\sigma}{\partial v_{rel}^2} \cdot \Delta v_{rel}^2 \qquad [4]$$

$\frac{\partial\sigma}{\partial v_{rel}}$ affects primarily the rotation measurement, resulting in an apparent rotation, whilst $\frac{\partial^2\sigma}{\partial v_{rel}^2}$ affects the Doppler width and hence the measurement of the ion temperature. The effective emission cross section dependence on the impact energy is plotted in figure 4. The diagram is based on a number of theoretical and experimental cross sections (Fritsch 1984,1989, Ryufuku 1982, Summers et al. 1990) The impact energy of the deuterium atoms can be classically written:

$$E_{imp} = \frac{M_D \mathbf{v_{rel}^2}}{2} \qquad [5]$$

where $\mathbf{v_{rel}} = \mathbf{v_D} - \mathbf{v_C}$, M_D is the mass of deuterium atom, $\mathbf{v_D}$ the velocity of the deuterium atom and $\mathbf{v_C}$ the velocity of the carbon ion.

For beam energies at 40 keV/amu we are at point 1 on the curve in figure 4 and therefore ions with velocity in the opposite direction to the neutral beam (higher impact energy) will have an enhanced effective emission cross section whilst the ions moving in the same direction as the neutral beam will have a smaller effective emission cross section (von Hellermann et al. 1987, Howell et al. 1988, Core et al. 1989) This leads effectively to a red shift of the observed spectrum. Obviously, cross section effects will increase with higher ion temperatures, when the thermal velocities of the carbon ions are higher. The effect is also more pronounced for lighter impurities, like helium (von Hellermann et al. 1990), for which the thermal velocities are higher due to their lower mass. For a thorough analysis of the phenomena, the integral below, which predicts the rate of emission, $\epsilon(v)$, has to be evaluated:

$$\epsilon(v) = \int d^3\mathbf{v_C} \int d^3\mathbf{v_D} f_C(\mathbf{v_C}) f_D(\mathbf{v_D}) \sigma(|\mathbf{v_D} - \mathbf{v_C}|) |\mathbf{v_D} - \mathbf{v_C}| \delta(v - \mathbf{n} \cdot \mathbf{v_C}) \quad [6]$$

The velocity distribution of the carbon ions can be approximated by a Maxwellian distribution shifted with the rotation velocity, v_{rot}, of the plasma

$$f_C = \frac{1}{\pi^{\frac{3}{2}} v_{th}^3} exp(-(\frac{v + v_{rot}}{v_{th}})^2) \quad [7a]$$

$$f_D(\mathbf{v}) = \delta(\mathbf{v} - \mathbf{v_k})\mathbf{v} \quad [7b]$$

The velocity distribution of the deuterium ions, f_D ,can be assumed to be discrete, i.e. the deuterium atoms have three different velocities $\mathbf{v_k}$, k=1,2,3 (2770 km/s, 1960 km/s and 1600 km/s respectively) due to the three energy components of the neutral beam. The cross section effects become important when the thermal velocities, v_{th}, of the carbon ions become comparable to these velocities.

The apparent rotation frequency induced by this red shift can then be calculated for different directions $\mathbf{n}$ (different angles between the line-of-sight and the neutral beam) and for different rotation velocities as a function of the ion temperature T_C. The cross sections needed for the calculations are taken from figure 4. The result, if only the first energy component is taken into account and the plasma is assumed to be at rest is shown in figure 5.

The amount of red shift depends mostly on the ion temperature and viewing geometry, but also slightly on the relative penetration of the three different neutral beam components contributing to the CX spectrum and on the plasma rotation, all according to [6]. In order to obtain the total red shift, the individual spectral lines for the three energy components in the neutral beam have to be calculated and added together. The positions of the three energy components are indicated with 1,2 and 3 in figure 4. The three Gaussian distributions, which have to be added, are shown in figure 6, where it can be seen that the second and third energy component give rise to small intensity but more significant red shift.

In figure 10 the total expected apparent rotation frequency caused by the red-shift has been evaluated according to the integral [6] with plasma parameters from 16 different time slots chosen from 10 pulses at JET (i.e. one or two times per pulse).

Extraction of central rotation frequency for the XCS

The XCS collects light along a line-of-sight cutting the plasma twice according to figure 1. The emissivity of the helium-like nickel would ideally be zero everywhere except for the absolute center of the plasma. The measured rotation velocity $v(\Delta\lambda)$ as a function of the Doppler shift $\Delta\lambda$ would then, according to formula [2], be:

$$\omega(\Delta\lambda) = c \cdot \frac{\Delta\lambda}{\lambda_0} \cdot \frac{1}{R_L} \qquad [8]$$

R (=3.05 m) is the major radius of the plasma and R_L (=1.82 m) is the distance of closest approach between the center of the torus and the line-of-sight (the minor radius of the plasma, a, is about 1.25 m).

The real situation is of course not this simple. The observed spectrum $I(\lambda)$ is instead obtained by summing spectra along the line-of-sight (Zastrow 1990). The line profiles are a convolution of a Gaussian line profile $\frac{I_G(\zeta,t)}{\sqrt{T_i(r)}}$ (due to Doppler broadening of the line) and a Lorentzian line profile $I_L(\zeta - \lambda(r,t))$ (due to the natural line broadening). The expression for $I(\lambda)$ then becomes

$$I(\lambda) = \int_{t}^{t+\Delta t} \int_{R_L}^{R+a} \int_{-\infty}^{\infty} k \cdot \epsilon(r) \frac{r}{\sqrt{(r^2 + R_L^2)}} \frac{I_G(\zeta, t)}{\sqrt{T_i(r)}} I_L(\zeta - \lambda(r,t)) d\zeta dr dt \quad [9]$$

The spectrum we observe is thus an average weighted towards the plasma center, where the emissivity, $\epsilon(r)$, is usually strongest. The weight function with the normalisation constant k in expression [9] is:

$$\int_{R_L}^{R+a} k \cdot \frac{\epsilon(r)}{\sqrt{T_i(r)}} \frac{r}{\sqrt{(r^2 + R_L^2)}} dr \quad [10]$$

The rotation frequency and ion temperature which are deduced from the resonance line without taking the emissivity profile into account will thus be an average rotation frequency and an average ion temperature. It is, however, possible to deduce the central values for rotation frequency and ion temperature measured by XCS from the observed spectrum $I(\lambda)$. The emissivity $\epsilon(r)$ of the resonance line as a function of major radius (r) is (Zastrow et al. 1991)

$$\epsilon(r) = n_e(r) \cdot n_{Ni}(r) \cdot \epsilon_{eff}(T_e(r)) \quad [11]$$

where n_e is the electron density, n_{Ni} is the nickel density, $T_e(r)$ is the electron temperature and ϵ_{eff} is the effective rate coefficient for the emissivity of the resonance line, which includes the fractional abundance of helium-like nickel. Using this in [10] enables the extraction of the rotation frequency in the center of the plasma and the central ion temperature. In order to do so we need to know the central values and the radial profile of the electron temperature and the electron density. We also need to know the gradients of the radial ion temperature profile and the radial profile of the toroidal rotation frequency. Then, the data from the charge exchange CXRS system can be compared with these extracted central XCS data.

When the information above is provided we have all the parameters we need to determine the integral [9]. Since the spectrum $I(\lambda)$ in the equation is known from a measurement it is possible to evaluate the central angular frequency and the central ion temperature. The integral

can be approximated with a sum over 50 different positions in the plasma. At each position the emissivity according to [11] is calculated. The central rotation frequency ω_{max} and the central ion temperature $T_{i,max}$ can be extracted by checking which input values of these parameters actually give the best fit to the measured spectrum $I(\lambda)$. This is done with an iterative procedure. The results for pulse number 19468 at 53.0 s are shown in figures7 and 8. The correction for the ion temperature (fig 7) is 1.1 keV upwards compared to the averaged value and the correction for the rotation (fig 8) is 33 krad/s upwards compared to the averaged value. For comparison, the rotation frequency profile and the ion temperature profile measured by charge exchange spectroscopy are also shown.

4.0 Results

In figure 9 the averaged and extracted central values of the ion temperature from XCS compared to the ion temperatures from CXRS are shown. It can be seen that the difference between these values can be very significant. Also the correction of charge exchange data for the cross section effect is indicated, which moves the data further towards the 45 degree line.

The experimental difference of the extracted central rotation frequency from XCS and that from CXRS and the theoretically predicted apparent rotation frequency caused by cross section effects shown in figure 10 is clearly of the same order. The discrepancy which can be seen when comparing to the theoretically predicted apparent rotation is an experimentally slightly larger difference. Possible explanations for this discrepancy are dicussed in the next section.

The data needed to get the figures 9 and 10 has been taken from 10 different pulses at JET for different times (one or two time slots per pulse) when the raw data were of good quality and the information provided by other diagnostics needed for the analysis of the x-ray data were available. For the XCS data each spectrum has been checked visually, and for the CXRS data selection has been based on penetration of the first energy component of the neutral beam to be in excess of 20% in the centre of the plasma. Since the nickel signal is usually increasing with time during a JET pulse whilst the penetration of the neutral beam usually decreases with time, a trade-off has to be made. The compromise has often meant to choose data from the middle part of the pulses. To get data for low ion temperatures some data had to be taken from the beginning of some pulses for which the nickel signal was not too low.

The errors due to lower count rate statistics are, however, only slightly higher for these pulses.

5.0 Discussion of possible error sources

Error sources in charge exchange spectroscopy

The error sources in the charge exchange spectroscopy measurement are count rate statistics, line-of-sight (plume-) effects and shift of the reference peak caused by rotation.

The error caused by count rate statistics is of the order of ±5 krad/s for the rotation frequency and about ±5 % for the ion temperature.

The prompt CXRS signal of the observed n=8 to n=7 transition in carbon is emitted at the intersection of the line-of-sight and the neutral beam (figure 1). This transition is, however, also to a minor extent emitted from C^{5+} ions drifting into the line-of-sight before getting re-ionised. This, so called plume effect, could, in cases where the charge exchange signal is poor, disturb the measurement of rotation frequency and ion temperature.

In some cases, for example during hot ion mode plasmas, the cold C^{5+} line used as a reference line is no longer stationary and can be subject to a slight shift. For this reason the Be^{1+} line at 5270.5 Å is, if possible, used as a fiducial wavelength (figure 3) and such pulses are checked individually by inspection.

The order of the error of the rotation frequency measured by charge exchange spectroscopy is thus ±5 krad/s and less than 10 % for the ion temperature.

Error sources in the x-ray crystal spectroscopy

In order to calibrate the wavelength scale of the x-ray crystal spectrometer the position of the w-line during pure Ohmic heating (no radio frequency or neutral beam heating) has been investigated. This position has been assumed to be the position of zero rotation. However,

the rotation frequency during Ohmic heating has been measured to be in the negative direction (counter to the plasma current) of the order 5 krad/s (Giannella 1988). This may partly explain the slightly larger experimental difference in figure 10 compared to the theoretical values.

The error of the central angular frequency measured by the XCS depends on count rate statistics and on errors in the central values and profiles of electron temperature, electron density, rotation frequency profile and ion temperature. All together this results in an uncertainty of the extracted central rotation frequency ω_{max} from the x-ray crystal spectrometer of 5 krad/s. The uncertainty in the ion temperature is around 20 %. For a detailed error analysis, see Zastrow et al. (1991).

6.0 Conclusions

The investigation of the cross section energy dependence of impact energy in active charge exchange spectroscopy and the emission profile of helium-like nickel in high resolution x-ray spectroscopy has lead to a significantly improved spectral analysis. For the analysis of the x-ray spectrum the electron temperature profiles from electron cyclotron emission or from Thomson scattering, and the electron density profiles from the laser interferometry measurements or Thomson scattering are reliable enough to make it possible to calculate the emissivity of the helium-like nickel in the plasma as a function of major radius.

A comparison between the central rotation frequencies from high resolution x-ray spectroscopy and rotation frequency from charge exchange spectroscopy (uncorrected for cross section effects) shows that the central rotation from x-ray spectroscopy is about 15% higher. The theoretically predicted deviation caused by the cross section variation is of the same order and in the same direction. All in all, the progress in understanding of the impact of the emission processes on the measurements leads to a much better agreement between the two diagnostic systems. For plasmas with broad electron temperature profiles and peaked ion and rotation frequency profiles the discrepancy used to be of the order of 60%. With the emission profiles and the cross section effect taken into account the agreement of inferred central values of the high resolution x-ray and the active charge exchange spectroscopy diagnostics at JET is within 5% for rotation frequency and within 20% for the ion temperature for all plasma scenarios.

Acknowledgements

We would like to thank Dr Paul Thomas for encouraging the development of ion temperature and plasma rotation diagnostics at JET.

We would also like to thank Dr Ralf König for fruitful discussions.

Finally we would like to thank B. Viaccoz and J. Holm for technical support, R. Barnsley for expertise and participation in improving the detector and crystal performance and J. Ellis and E. Oord for programming support.

References

H. Biglari, P.H. Diamond and P.W. Terry, Phys. Fluids **b2** (1991) 1

F. Bombarda, R. Giannella, E. Källne and G.J. Tallents, J. Quant. Spectrosc. Radiat. Transfer **41**, 323 (1989)

W.G.F. Core and N. Cowern, "Influence of neutral beam injection on the velocity distribution of excited atoms in a plasma", JET-P(89)11

L.G. Eriksson, R. Giannella, T. Hellsten, E. Källne, G. Sundström, "Observations of toroidal plasma rotation induced by ICRH at JET", submitted to Plasma Physics and Controlled Fusion, 1990

H.P.L. de Esch, D. Stork and H. Weisen, 17^{th} EPS conf. on Plasma Physics and Controlled Fusion, Amsterdam, 1990

W. Fritsch, Phys.Rev. **A29**, 3039 (1984)

W. Fritsch, 1989, J.Phys.Coll **50**, 87 (1989)

R. Giannella, J. de Physique **49**, C1-283 (1988)

R.J. Groebner et al., Phys. Rev. Lett. **63**, 2369 (1989)

R.J. Groebner et al., 13^{th} IAEA Conf., Washington D.C., USA, paper A-6-4 (1990)

M.G. von Hellerman et al., IEA Large Tokamak Workshop on Ion Temperature Measurements, PPL Princeton N.J., Nov 1987

M.G. von Hellermann, A. Boileau, W. Mandl, H.P. Summers, J. Friedling, "Investigation of thermal and slowing down alpha particles using charge exchange spectroscopy" to appear in Nuclear Fusion

M.G. von Hellermann, W. Mandl, H.P. Summers, H. Weisen, A. Boileau, P.D. Morgan, H.W. Morsi, R. König, M.F. Stamp and R. Wolf, Rev. Sci. Instr. **61**, 3479 (1990)

R.B. Howell, R.J. Fonck, R.J. Knize, K.P. Jaehnig, Rev. Sci. Ins., **59**, 1521 (1988)

H. Morsi, M.G. von Hellermann, R. Barnsley et al., 17^{th} EPS conf. on Plasma Physics and Controlled Fusion, Amsterdam 1990

M.F.F. Nave and J.A. Wesson, "Mode locking in tokamaks", to appear in Nuclear Fusion (1991)

H. Ryufuku, JAERI 5182, 031 (1982)

K.C. Shaing and E.C. Crume, Phys. Rev. Lett. **63**, 2365 (1989)

J. Snipes, D.J.Campbell, T.C. Hender et al., Nucl. Fusion **30**, 205 (1990)

H.P. Summers, R. Giannella, M.G. von Hellerman et al., "JET Spectra and their Interpretation",in Atomic Spectra and Oscillator Strength for Astrophysics and Fusion, to be published by North Holland Publ(1990)

H. Weisen, M.G. von Hellermann, A. Boileau, L.D. Horton, W. Mandl, H.P. Summers,
Nuclear Fusion **29**, 2187 (1989)

K.-D. Zastrow, E. Källne, H.P. Summers Phys.Rev. **A41**, 1427 (1990)

K.-D. Zastrow, H.W. Morsi, M. Danielsson, M.G. von Hellermann, E. Källne, R. König and W. Mandl, "Deduction of central plasma parameters from line-of-sight averaged spectroscopic observations", JET-P(90)18, submitted to Phys. Rev. (1991)

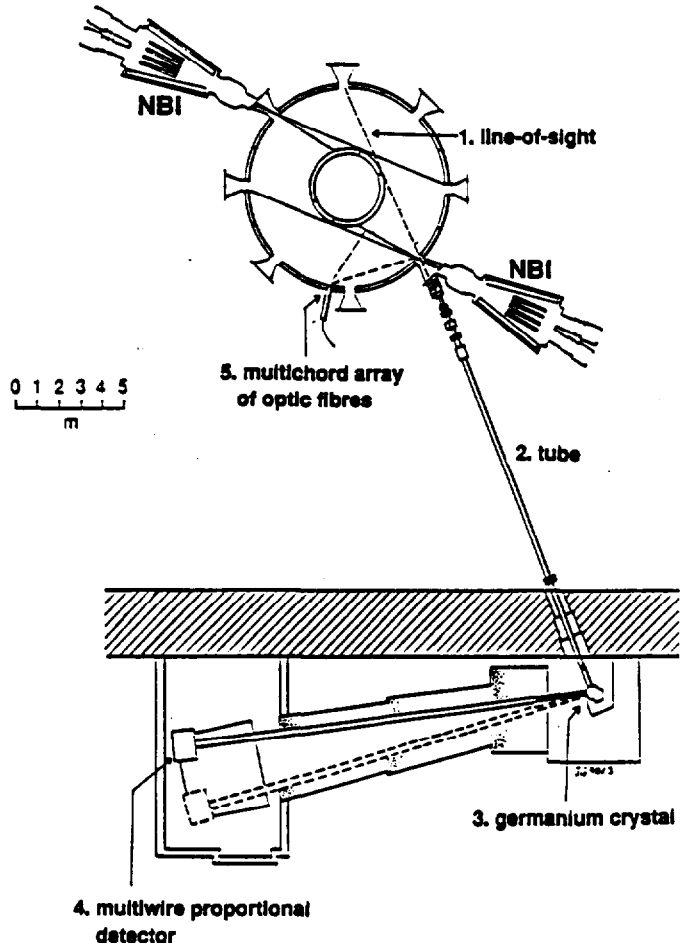

Figure 1 Set-up of the high resolution x-ray crystal spectrometer (XCS) and the charge exchange multichord system (CXRS) with the neutral beam injectors (NBI) around the JET torus.

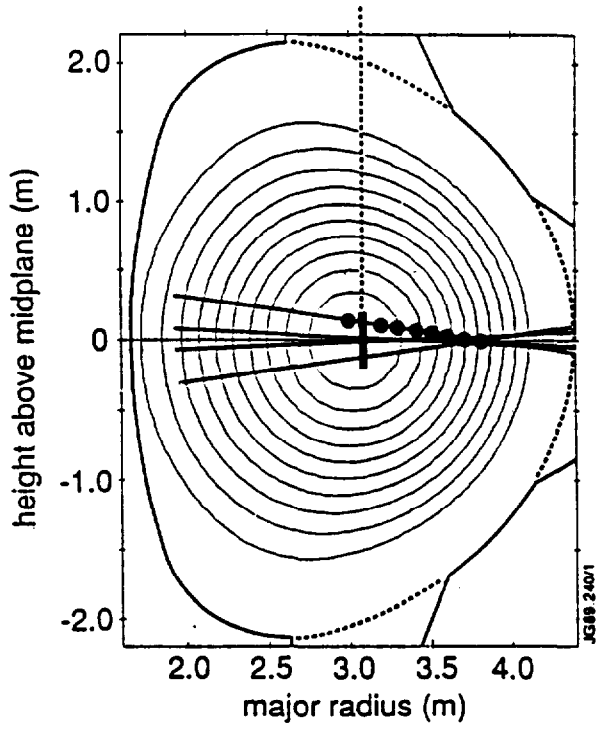

Figure 2

Points of measurement along the major radius for the CXRS

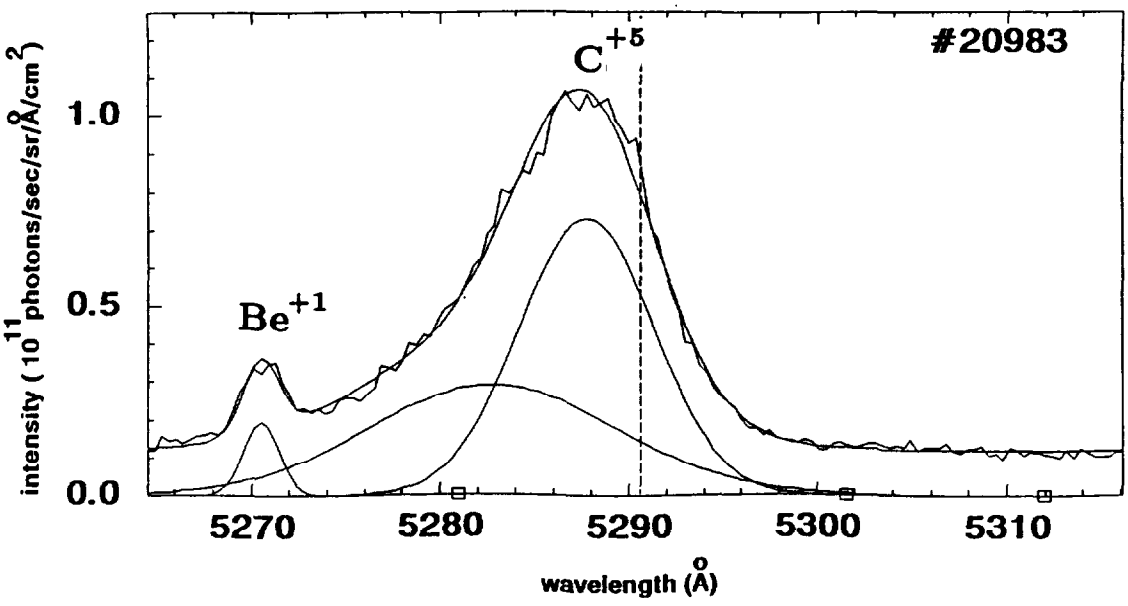

Figure 3

Carbon charge exchange recombination spectrum as observed with the central chord of the CXRS. The line indicates the unshifted position of the carbon line.

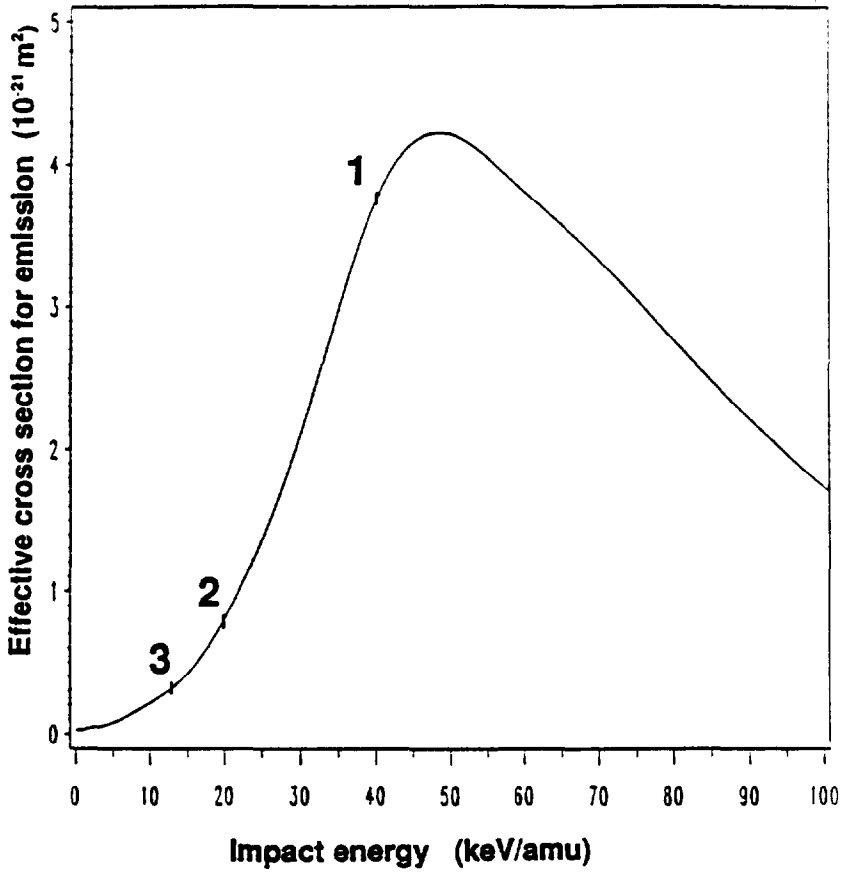

Figure 4

Effective emission cross section variation with impact energy for emission for the C^{5+} n=8 to n=7 transition

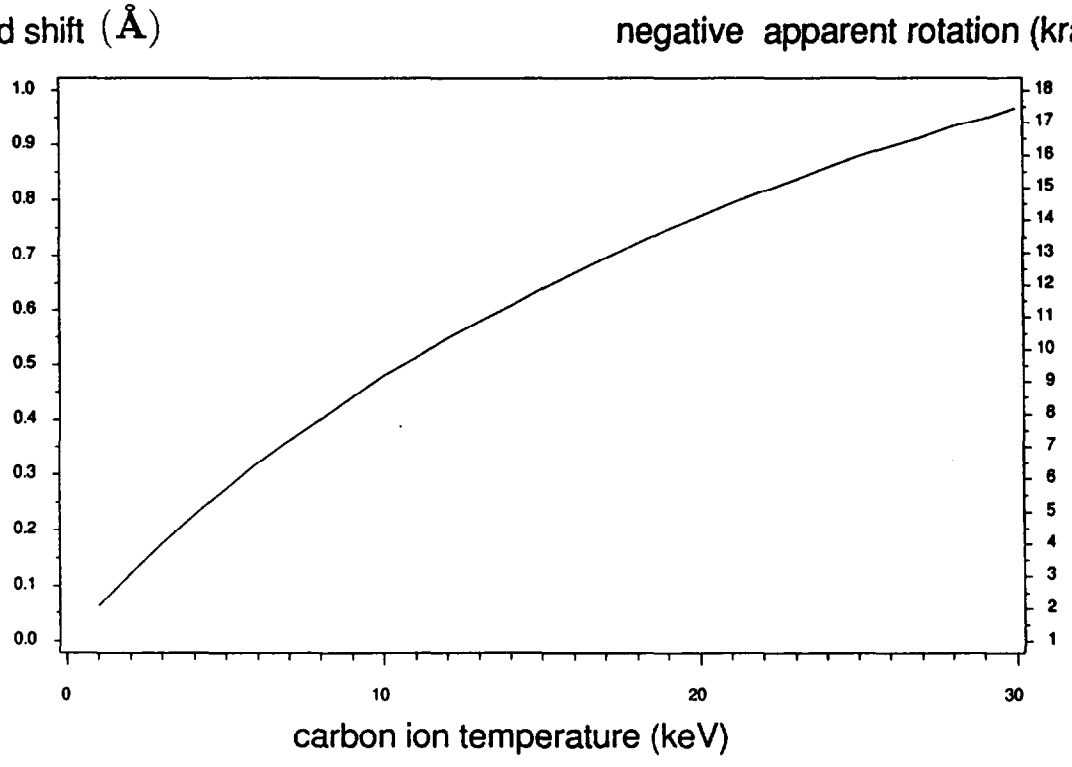

Figure 5

Red shift and the connected apparent rotation induced by cross section effects for the first energy component of the neutral beam as a function of ion temperature for the angle between line-of-sight and neutral beam corresponding to the plasma center, assuming that the plasma is at rest

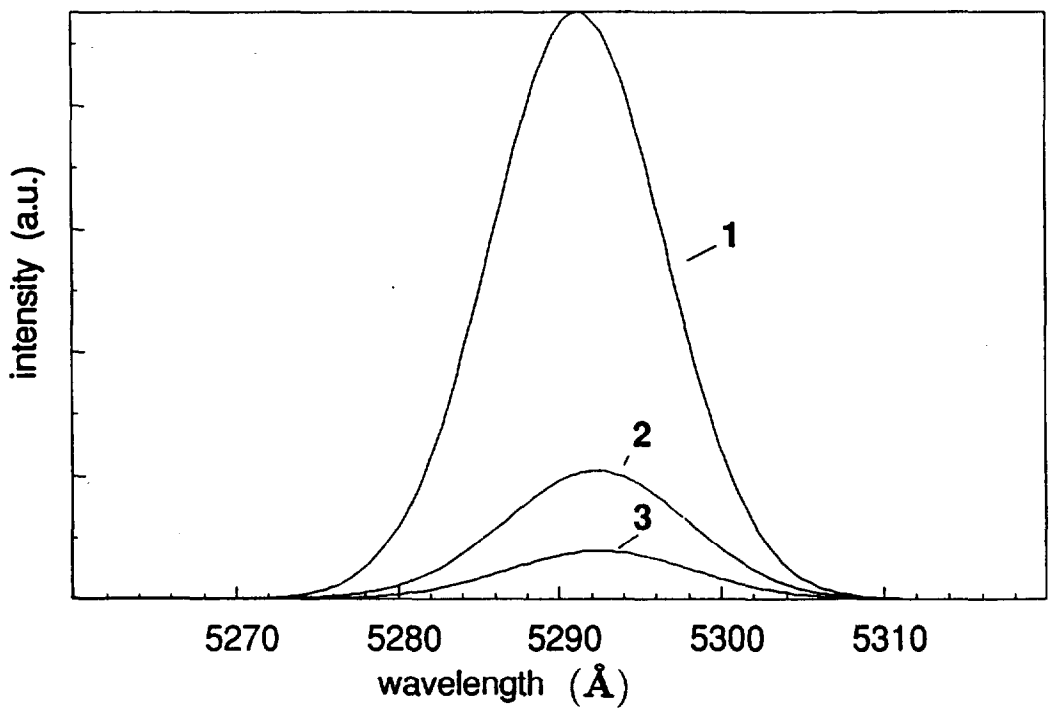

Figure 6

Simulated spectral lines due to charge exchange with the different energy components of the neutral beam.

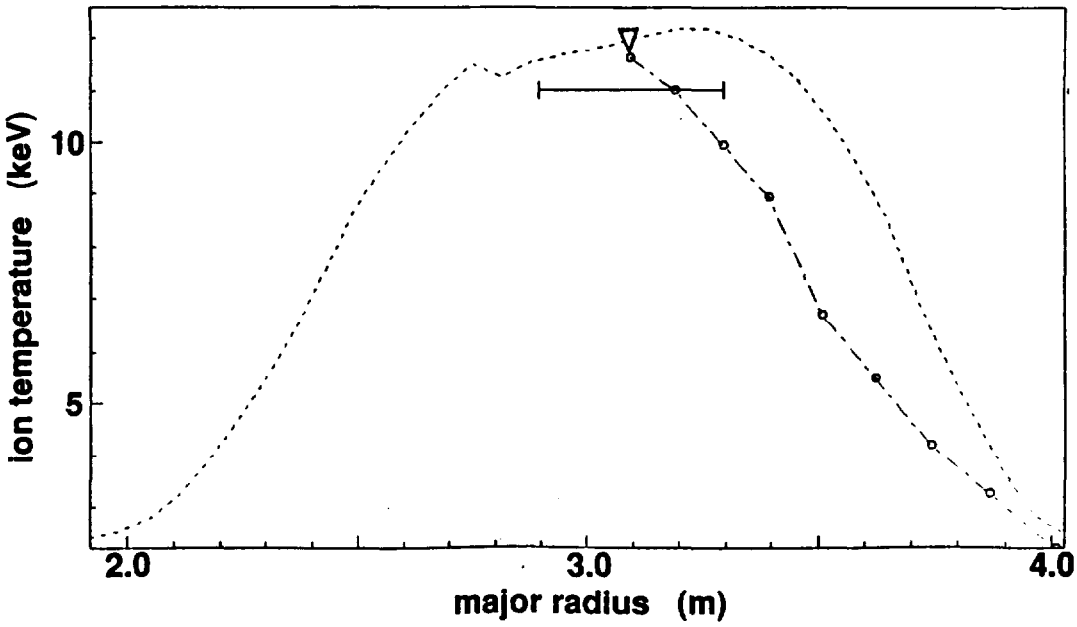

Figure 7

Extracted central ion temperature from XCS (▽), averaged ion temperature from XCS (⊢⊣), ion temperature profile used for the iterations (·--·) and ion temperature profile from charge exchange (⊢·-·) for JET discharge number 19462.

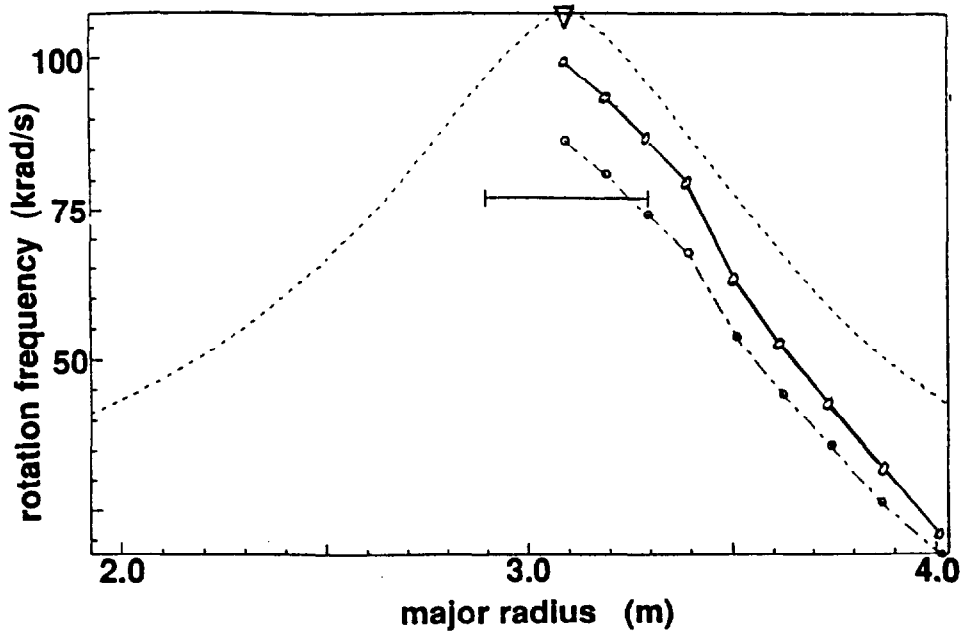

Figure 8

Extracted central rotation frequency from the XCS (▽), averaged rotation frequency from the XCS (⊢⊣), rotation frequency profile used for the iterations (·--·) and rotation frequency profile from charge exchange spectroscopy (⊢·-·) for JET discharge number 19462.

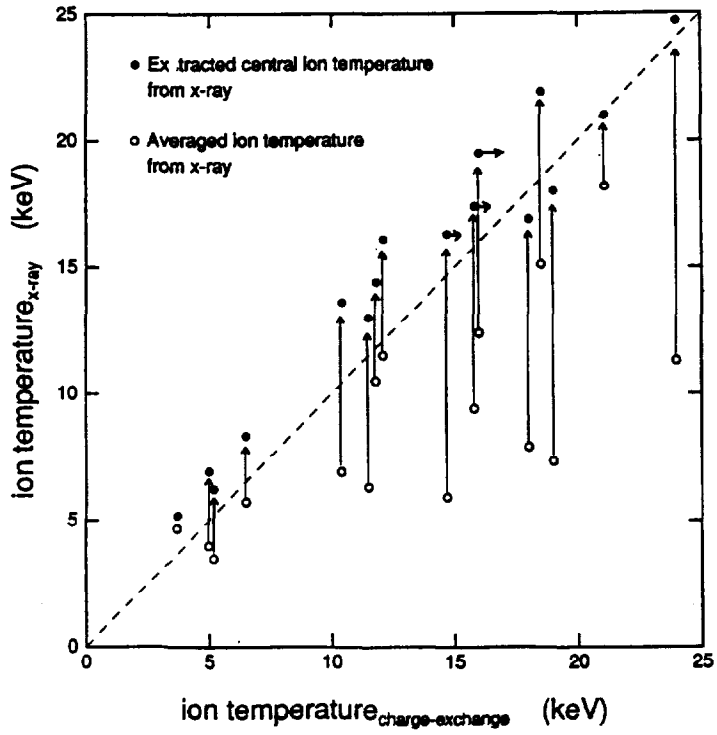

Figure 9

Averaged ion temperature and extracted central ion temperature from XCS compared to CXRS ion temperature.

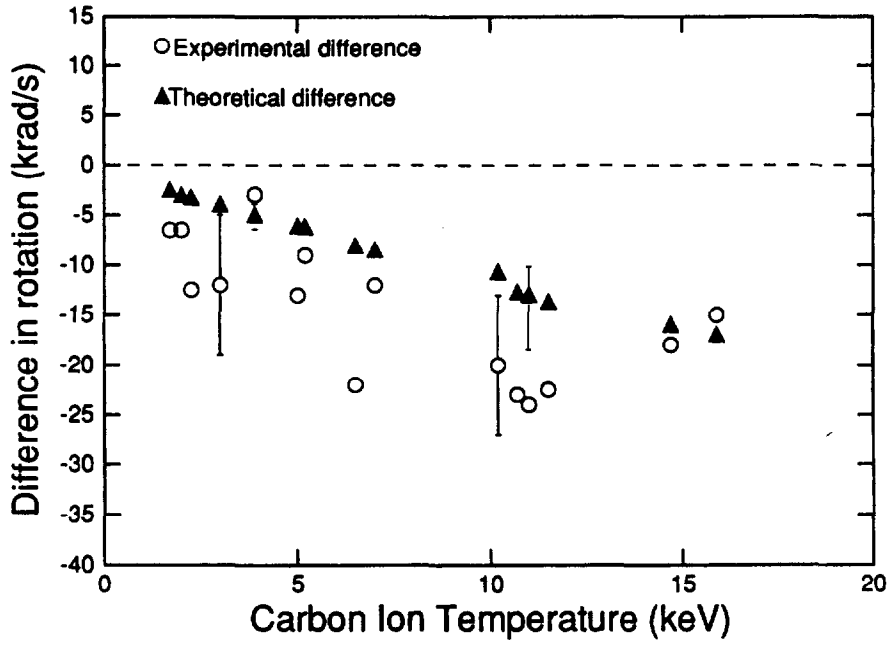

Figure 10

Experimental difference in central rotation frequency data from CXRS and central rotation frequency from XCS plotted against ion temperature together with the theoretically predicted difference. Typical error bars are shown for both experimental and theoretical data. The latter are asymmetrical as a result of neglecting the real plasma rotation (v_{rot} in [7a]) in the calculations.

APPENDIX 1.

THE JET TEAM

JET Joint Undertaking, Abingdon, Oxon, OX14 3EA, U.K.

J.M.Adams[1], F.Alladio[4], H.Altmann, R.J.Anderson, G.Appruzzese, W.Bailey, B.Balet, D.V.Bartlett, L.R.Baylor[24], K.Behringer, A.C.Bell, P.Bertoldi, E.Bertolini, V.Bhatnagar, R.J.Bickerton, A.Boileau[3], T.Bonicelli, S.J.Booth, G.Bosia, M.Botman, D.Boyd[31], H.Brelen, H.Brinkschulte, M.Brusati, T.Budd, M.Bures, T.Businaro[4], H.Buttgereit, D.Cacaut, C.Caldwell-Nichols, D.J.Campbell, P.Card, J.Carwardine, G.Celentano, P.Chabert[27], C.D.Challis, A.Cheetham, J.Christiansen, C.Christodoulopoulos, P.Chuilon, R.Claesen, S.Clement[30], J.P.Coad, P.Colestock[6], S.Conroy[13], M.Cooke, S.Cooper, J.G.Cordey, W.Core, S.Corti, A.E.Costley, G.Cottrell, M.Cox[7], P.Cripwell[13], F.Crisanti[4], D.Cross, H.de Blank[16], J.de Haas[16], L.de Kock, E.Deksnis, G.B.Denne, G.Deschamps, G.Devillars, K.J.Dietz, J.Dobbing, S.E.Dorling, P.G.Doyle, D.F.Düchs, H.Duquenoy, A.Edwards, J.Ehrenberg[14], T.Elevant[12], W.Engelhardt, S.K.Erents[7], L.G.Eriksonn[5], M.Evrard[2], H.Falter, D.Flory, M.Forrest[7], C.Froger, K.Fullard, M.Gadeberg[11], A.Galetsas, R.Galvao[8], A.Gibson, R.D.Gill, A.Gondhalekar, C.Gordon, G.Gorini, C.Gormezano, N.A.Gottardi, C.Gowers, B.J.Green, F.S.Griph, M.Gryzinski[26], R.Haange, G.Hammett[6], W.Han[9], C.J.Hancock, P.J.Harbour, N.C.Hawkes[7], P.Haynes[7], T.Hellsten, J.L.Hemmerich, R.Hemsworth, R.F.Herzog, K.Hirsch[14], J.Hoekzema, W.A.Houlberg[24], J.How, M.Huart, A.Hubbard, T.P.Hughes[32], M.Hugon, M.Huguet, J.Jacquinot, O.N.Jarvis, T.C.Jernigan[24], E.Joffrin, E.M.Jones, L.P.D.F.Jones, T.T.C.Jones, J.Källne, A.Kaye, B.E.Keen, M.Keilhacker, G.J.Kelly, A.Khare[15], S.Knowlton, A.Konstantellos, M.Kovanen[21], P.Kupschus, P.Lallia, J.R.Last, L.Lauro-Taroni, M.Laux[33], K.Lawson[7], E.Lazzaro, M.Lennholm, X.Litaudon, P.Lomas, M.Lorentz-Gottardi[2], C.Lowry, G.Magyar, D.Maisonnier, M.Malacarne, V.Marchese, P.Massmann, L.McCarthy[28], G.McCracken[7], P.Mendonca, P.Meriguet, P.Micozzi[4], S.F.Mills, P.Millward, S.L.Milora[24], A.Moissonnier, P.L.Mondino, D.Moreau[17], P.Morgan, H.Morsi[14], G.Murphy, M.F.Nave, M.Newman, L.Nickesson, P.Nielsen, P.Noll, W.Obert, D.O'Brien, J.O'Rourke, M.G.Pacco-Düchs, M.Pain, S.Papastergiou, D.Pasini[20], M.Paume[27], N.Peacock[7], D.Pearson[13], F.Pegoraro, M.Pick, S.Pitcher[7], J.Plancoulaine, J-P.Poffé, F.Porcelli, R.Prentice, T.Raimondi, J.Ramette[17], J.M.Rax[27], C.Raymond, P-H.Rebut, J.Removille, F.Rimini, D.Robinson[7], A.Rolfe, R.T.Ross, L.Rossi, G.Rupprecht[14], R.Rushton, P.Rutter, H.C.Sack, G.Sadler, N.Salmon[13], H.Salzmann[14], A.Santagiustina, D.Schissel[25], P.H.Schild, M.Schmid, G.Schmidt[6], R.L.Shaw, A.Sibley, R.Simonini, J.Sips[16], P.Smeulders, J.Snipes, S.Sommers, L.Sonnerup, K.Sonnenberg, M.Stamp, P.Stangeby[19], D.Start, C.A.Steed, D.Stork, P.E.Stott, T.E.Stringer, D.Stubberfield, T.Sugie[18], D.Summers, H.Summers[20], J.Taboda-Duarte[22], J.Tagle[30], H.Tamnen, A.Tanga, A.Taroni, C.Tebaldi[23], A.Tesini, P.R.Thomas, E.Thompson, K.Thomsen[11], P.Trevalion, M.Tschudin, B.Tubbing, K.Uchino[29], E.Usselmann, H.van der Beken, M.von Hellermann, T.Wade, C.Walker, B.A.Wallander, M.Walravens, K.Walter, D.Ward, M.L.Watkins, J.Wesson, D.H.Wheeler, J.Wilks, U.Willen[12], D.Wilson, T.Winkel, C.Woodward, M.Wykes, I.D.Young, L.Zannelli, M.Zarnstorff[6], D.Zasche[14], J.W.Zwart.

PERMANENT ADDRESS

1. UKAEA, Harwell, Oxon. UK.
2. EUR-EB Association, LPP-ERM/KMS, B-1040 Brussels, Belgium.
3. Institute National des Récherches Scientifique, Quebec, Canada.
4. ENEA-CENTRO Di Frascati, I-00044 Frascati, Roma, Italy.
5. Chalmers University of Technology, Göteborg, Sweden.
6. Princeton Plasma Physics Laboratory, New Jersey, USA.
7. UKAEA Culham Laboratory, Abingdon, Oxon. UK.
8. Plasma Physics Laboratory, Space Research Institute, Sao José dos Campos, Brazil.
9. Institute of Mathematics, University of Oxford, UK.
10. CRPP/EPFL, 21 Avenue des Bains, CH-1007 Lausanne, Switzerland.
11. Risø National Laboratory, DK-4000 Roskilde, Denmark.
12. Swedish Energy Research Commission, S-10072 Stockholm, Sweden.
13. Imperial College of Science and Technology, University of London, UK.
14. Max Planck Institut für Plasmaphysik, D-8046 Garching bei München, FRG.
15. Institute for Plasma Research, Gandhinagar Bhat Gujat, India.
16. FOM Instituut voor Plasmafysica, 3430 Be Nieuwegein, The Netherlands.
17. Commissiariat à L'Energie Atomique, F-92260 Fontenay-aux-Roses, France.
18. JAERI, Tokai Research Establishment, Tokai-Mura, Naka-Gun, Japan.
19. Institute for Aerospace Studies, University of Toronto, Downsview, Ontario, Canada.
20. University of Strathclyde, Glasgow, G4 ONG, U.K.
21. Nuclear Engineering Laboratory, Lapeenranta University, Finland.
22. JNICT, Lisboa, Portugal.
23. Department of Mathematics, Univeristy of Bologna, Italy.
24. Oak Ridge National Laboratory, Oak Ridge, Tenn., USA.
25. G.A. Technologies, San Diego, California, USA.
26. Institute for Nuclear Studies, Swierk, Poland.
27. Commissiariat à l'Energie Atomique, Cadarache, France.
28. School of Physical Sciences, Flinders University of South Australia, South Australia SO42.
29. Kyushi University, Kasagu Fukuoka, Japan.
30. Centro de Investigaciones Energeticas Medioambientales y Techalogicas, Spain.
31. University of Maryland, College Park, Maryland, USA.
32. University of Essex, Colchester, UK.
33. Akademie de Wissenschaften, Berlin, DDR.

CR 88.49.1A